Electron Transfer in Phenothiazine/Ru(bpy)$_3^{2+}$ Donor−Chromophore Complexes

S. L. Larson,† C. Michael Elliott,* and D. F. Kelley*

Department of Chemistry, Colorado State University, Fort Collins, Colorado 80523

Received April 20, 1995[⊗]

Time-resolved emission studies have been performed on a series of covalently linked Ru(bipyridine)$_3$−phenothiazine complexes. The emissive Ru(bipyridine)$_3$ metal-to-ligand charge-transfer (MLCT) excited state is quenched by electron donation from a phenothiazine (PTZ) donor. The rates of electron transfer (ET) to the MLCT states from the PTZ donor have been analyzed in terms of Marcus theory, in which each phenothiazine acts independently of other phenothiazines in the complex. Reaction energetics were determined from electrochemical data for Ru(2+/1+) and PTZ(1+/0) reduction potentials and MLCT state energies. Quantitative agreement was found between the model's predictions and measured ET times. The results are compared to those obtained for the analogous electron transfer leading to charge separated state formation in a related donor−chromophore−acceptor system.

Introduction

The dynamics of electron transfer are known to depend on the structure of the reactants, the distance separating the reactants, the nature and polarity of the medium, and Coulombic effects. A number of important advances in the theory of electron-transfer reactions have been made by Marcus, Hush, Jortner, and Bixon among others.[1−13] Experimental investigations of electron-transfer dynamics allow for testing of theory as well as modeling more complex systems such as the biological processes of respiration and photosynthesis.[14,15] Intramolecular electron transfer reactions are of particular interest, since intramolecular electron transfer between an excited-state chromophore and an electron donor or acceptor is often quite efficient.[16−37]

We have previously studied intramolecular electron-transfer reactions involving tris(bipyridine)ruthenium(II), [Ru(bpy)$_3$]$^{2+}$.[30,34,37] The lowest energy excited state of the Ru(bpy)$_3^{2+}$ chromophore is metal-to-ligand charge transfer (MLCT) in nature, where one of the metal d electrons has been promoted into a bipyridine-based π^* orbital. The MLCT excited state is easily oxidized or reduced and may be quenched by either electron donors or acceptors. Both types of reactions are of interest.

Our initial studies involved molecules in which the Ru(bpy)$_3^{2+}$ chromophore is covalently linked to a diquat electron acceptor.[30,34a−c] Subsequently, studies were conducted on more complicated molecules consisting of a Ru(bpy)$_3^{2+}$ chromophore,

* To whom correspondence should be addressed.
† Current address: Army Corps of Engineers, Waterways Experiment Station, Vicksburg, MS 39180.
⊗ Abstract published in *Advance ACS Abstracts,* February 15, 1996.

(1) *Photo Induced Electron Transfer*; Fox, M. A., Chanon, M., Eds.: Elsevier: Amsterdam, 1988, and text references therein.
(2) Hush, N. S. *Trans. Faraday Soc.* **1961**, *57*, 155.
(3) Marcus, R. A. *Discuss. Faraday Soc.* **1960**, *29*, 21.
(4) Meyer, T. J. *Top. Curr. Chem.* **1990**, *156*, 388−440.
(5) Sutin, N. *Top. Curr. Chem.* **1990**, *156*, 441.
(6) Kavarnos, G. J. *Top. Curr. Chem.* **1990**, *156*, 22−58.
(7) Marcus, R. A. *Annu. Rev. Phys. Chem.* **1964**, *15*, 155.
(8) Marcus, R. A. *Electrochim. Acta* **1968**, *13*, 995.
(9) German, E. D.; Dvali, V. G.; Dogonadze, R. R.; Kuznetsov, A. M. *Elektrakimiya* **1976**, *12*, 639.
(10) Creutz, C.; Kroger, P.; Matsabura, T. L.; Netzel, T. L.; Sutin, N. *J. Am. Chem. Soc.* **1979**, *101*, 5442.
(11) Ulstrop, J.; Jortner, J. *J. Phys. Chem.* **1975**, *63*, 4358.
(12) Efrima, S.; Bixon, M. *J. Phys. Chem.* **1952**, *20*, 1752.
(13) Ulstrup, J. *Charge Transfer in Condensed Media*; Springer-Verlag: Berlin, 1979, and text references therein.
(14) Meyer, T. J. *Acc. Chem. Res.* **1989**, *22*, 5.
(15) *Photochemical Conversion and Storage of Solar Energy*; Connolly, J. S., Ed.; Academic Press: New York, 1981.
(16) Closs, G. L.; Miller, J. R. *Science* **1988**, *240*, 440
(17) Marcus, R. A.; Sutin, N. *Biochem. Biophys. Acta* **1985**, *265*, 811.
(18) Guarr, T.; McLendon, G. *Coord. Chem. Rev.* **1985**, *68*, 1.
(19) Hush, N. S. *Coord. Chem. Rev.* **1985**, *64*, 135.
(20) Closs, G. L.; Piotowiak, P.; MacKinnis, J. M.; Fleming, G. R. *J. Am. Chem. Soc.* **1988**, *110*, 2652.
(21) Calcaterra, L. T.; Closs, G. L.; Miller, L. R. *J. Am. Chem. Soc.* **1984**, *115*, 670.
(22) Oliver, A. M.; Craig, D. C.; Paddon-Row, M. N.; Kroon, J.; Verhoeven, J. W. *Chem. Phys. Lett.* **1988**, *150*, 366.
(23) Oevering, H.; Paddon-Row, M. N.; Heppener, M.; Oliver, A. M.; Cotsaris, E.; Verhoeven, J. W.; Hush, N. S. *J. Am. Chem. Soc.* **1987**, *109*, 3258.
(24) Kroon, J.; Oliver, A. M.; Padden-Row, M. N. *Recl. Trav. Chim. Pays-Bas* **1988**, *107*, 509.
(25) Verhoeven, J. W.; Paddon-Row, M. N.; Hush, N. S.; Oevering, M.; Heppener, M. *Pure Appl. Chem.* **1986**, *58*, 1285.
(26) Gust, D.; Moore, T. A.; Moore, A. L.; Leggett, L.; Lin, S.; Degraziano, J. M.; Hermant, R. M.; Nicodem, D.; Craig, P.; Seely, G. R.; Nieman, R. A. *J. Phys. Chem.* **1993**, *97*, 7926−7931.
(27) Yonemoto, E. H.; Riley, R. L.; Kim, Y. I.; Atherton, S. J.; Schmehl, R. H.; Mallouk, T. E. *J. Am. Chem. Soc.* **1993**, *115*, 5348.
(28) Jones, W. E.; Bignozzi, C. A.; Chen, P.; Meyer, T. J., *Inorg. Chem.* **1993**, *32*, 1167−1178.
(29) Yonemoto, E. H.; Riley, R. L.; Kim, Y. I.; Atherton, S. J.; Schmehl, R. H.; Mallouk, T. E. *J. Am. Chem. Soc.* **1992**, *114*, 8081−8087.
(30) Ryu, C. K.; Wang, R.; Schmehl, R. H.; Ferrere, S.; Ludwikow, M.; Merkert, J. W.; Headford, C. E. L.; Elliott, C. M. *J. Am. Chem. Soc.* **1992**, *114*, 430−438.
(31) Wasielewski, M. R. *Chlorophylls*; Scheer, H., Ed.; CRC: Boca Raton, FL, 1991; pp 269−286.
(32) MacQueen, D. B.; Schanze, K. S. *J. Am. Chem. Soc.* **1991**, *113*, 7470−7479.
(33) MacQueen, D. B.; Perkins, T. A.; Schmehl, R. H.; Schanze, K. S. *Mol. Cryst. Liq. Cryst.* **1991**, *194*, 113−121.
(34) (a) Schmehl, R. H.; Ryu, C. K.; Elliott, C. M.; Headford, C. L. E.; Ferrere, S. *Adv. Chem. Ser.* **1989**, *226*, 211−223. (b) Elliott, C. M.; Freitag, R. A.; Blaney, D. D. *J. Am. Chem. Soc.* **1985**, *107*, 4647−4655. (c) Cooley, L. F.; Headford, C. E. L.; Elliott, C. M.; Kelley, D. F. *J. Am. Chem. Soc.* **1988**, *110*, 6673−6682. (d) Danielson, E.; Elliott, C. M.; Merkert, J. W.; Meyer, T. J. *J. Am. Chem. Soc.* **1987**, *109*, 2519−2520. (e) Larson, S. L.; Cooley, L. F.; Elliott, C. M.; Kelley, D. F. *J. Am. Chem. Soc.* **1992**, *114*, 9504−9509.
(35) Cabana, L. A.; Schanze, K. S. *Adv. Chem. Ser.* **1989**, *226*, 101−124.
(36) Wasielewski, M. R.; Niemczyk, M. P.; Johnson, D. G.; Svec, W. A.; Minsek, D. W. *Tetrahedron* **1989**, *45*, 4785−4806.
(37) Cooley, L. F.; Larson, S. L.; Elliott, C. M.; Kelley, D. F. *J. Phys. Chem.* **1991**, *95*, 10694.
(38) Sawyer, D. T.; Roberts, J. L. *Experimental Electrochemistry for Chemists*; Wiley: New York, 1974.
(39) Sasse, W. H. F.; Whittle, C. P. *J. Am. Chem. Soc.* **1961**, *83*, 1347.

0020-1669/96/1335-2070$12.00/0

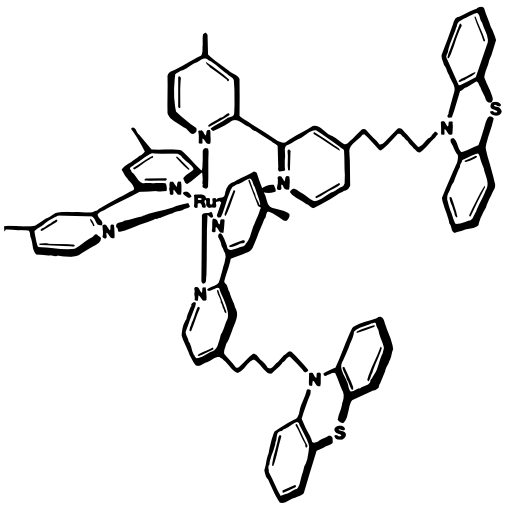

Figure 1. [Ru(44-PTZ)$_2$DMB]$^{2+}$ donor−chromophore complex.

a diquat electron acceptor, and a phenothiazine (PTZ) electron donor.[34d,e,37,40] These donor−chromophore−acceptor systems undergo two separate electron-transfer steps to form a long-lived charge-separated state. The MLCT state is initially quenched by electron transfer from the chromophore to the diquat electron acceptor, followed by rapid PTZ-to-Ru^{3+} electron transfer.

To further study the PTZ-to-ruthenium electron-transfer events, we have synthesized a series of molecules containing a Ru(bpy)$_3^{2+}$ chromophore and one or more phenothiazine electron donors. The electron-transfer dynamics of these donor−chromophore "diad" systems are presented here. Specifically, the phenothiazine electron donors are attached via variable-length methylene chains to a Ru(bpy)$_3^{2+}$ chromophore. Time-resolved emission spectroscopy is used to determine the reductive quenching rates. An example of a donor-chromophore complex containing two phenothiazine electron donors and a dimethylbipyridine (DMB) ligand, where the chromophore-to-phenothiazine linkage is four methylene units ($p = 4$, [Ru(4*p*-PTZ)$_2$(DMB)]$^{2+}$), is shown in Figure 1. Results of these investigations for donor−chromophore complexes are analyzed with an emphasis on the role of the solvent, electron-transfer distance, number of phenothiazine-containing ligands, and driving force for electron transfer.

Experimental Section

Measurements. Cyclic voltammetry was performed using either a PAR Model 173 potentiostat or a BAS100 electrochemical analyzer. All electrochemical measurements were carried out in oxygen-free, nitrogen-purged acetonitrile solutions with 0.1 M tetra-*n*-butylammonium hexafluorophosphate ((TBA)PF$_6$) as supporting electrolyte. A conventional three-electrode cell was used with a glassy-carbon or platinum working electrode, a platinum wire loop auxiliary electrode, and an SCE electrode as reference.

Chemicals and Solvents. All reagents and solvents were purchased and used without further purification, except as noted. Acetonitrile (Burdick and Jackson) for electrochemical measurements was degassed and stored under nitrogen and used without further purification. Tetra-*n*-butylammonium hexafluorophosphate ((TBA)PF$_6$) was prepared by metathesis of ammonium hexafluorophosphate and tetra-*n*-butylammonium iodide (TBAI) in acetone/water, followed by three recrystallizations from 95% ethanol as previously reported.[38] The electrolyte was dried for 24 h at 75 °C *in vacuo*.

4,4′-Dimethyl-2,2′-bipyridine (DMB). This compound was supplied by Reilly Tar and Chemical, Indianapolis, IN, and was recrystallized from ethyl acetate (colorless crystals, mp 172−177 °C) and dried *in vacuo* (24 h, room temperature) before use.

4,4′,5,5′-tetramethyl-2,2′-bipyridine (TMB). The ligand was prepared by conventional methods from 3,4-lutidine (Aldrich).[39] The product was recrystallized from ethyl acetate (colorless crystals, mp 248−250 °C).

***N*-Methylphenothiazine (Me-PTZ), 4-Methyl-4′-(3-(phenothiazino)propyl)-2,2′-bipyridine (43-PTZ), 4-Methyl-4′-(4-(phenothiazino)butyl)-2,2′-bipyridine (44-PTZ), 4-Methyl-4′-(5-(phenothiazino)pentyl)-2,2′-bipyridine (45-PTZ), 4-Methyl-4′-(6-(phenothiazino)hexyl)-2,2′-bipyridine (46-PTZ), 4-Methyl-4′-(7-(phenothiazino)heptyl)-2,2′-bipyridine (47-PTZ), and 4-Methyl-4′-(8-(phenothiazino)octyl)-2,2′-bipyridine (48-PTZ).** The preparation of these compounds has been reported previously.[40]

Ru(DMSO)$_4$Cl$_2$, Bis(DMB)dichlororuthenium(II) (Ru(DMB)$_2$Cl$_2$), Bis(TMB)dichlororuthenium(II), (Ru(TMB)$_2$Cl$_2$), Bis(bipyridine)-dichlororuthenium(II) (Ru(bpy)$_2$Cl$_2$), and Bis(4*p*-PTZ)dichlororuthenium (Ru(4*p*-PTZ)$_2$Cl$_2$). These ruthenium complexes were prepared as described previously.[40]

[Ru(DMB)$_2$(4*p*-PTZ)](PF$_6$)$_2$, [Ru(TMB)$_2$(4*p*-PTZ)](PF$_6$)$_2$, and [Ru(bipyridine)$_2$(4*p*-PTZ)](PF$_6$)$_2$. Throughout the procedure below, room light was excluded. A red glass test tube containing a mixture of Ru(bpy, DMB, or TMB)$_2$Cl$_2$ (30 mg) in 15 mL of ethylene glycol (under N_2) was placed in a paraffin bath at 120 °C for 30 min, after which the solution was cooled to room temperature. To the resulting red-orange solution was added 4*p*-PTZ (1 equiv), and this solution was then placed in the 120 °C paraffin bath for 30 min. The solution was cooled to room temperature, diluted 1:1 with distilled water, and filtered. Filtered, saturated aqueous NH_4PF_6 (2 mL) was added, and the resulting orange solid was isolated by centrifugation. Column chromatography on silica gel (eluent: 10% saturated aqueous KNO_3/40% water/50% acetonitrile) was used for purification. Acetonitrile was removed by rotary evaporation from those fractions containing only the desired product (as determined by TLC and UV−visible spectroscopy). Saturated aqueous NH_4PF_6 (2 mL) was added dropwise. The pure product was isolated by centrifugation, washed with 2 × 10 mL of distilled water, and dried *in vacuo* (24 h, overnight). Yields were typically 20−40%.

After chromatographic purification all samples were examined by cyclic voltammetry. The peak currents for the respective oxidation or reduction waves indicate a ratio of 1:1:1:1 for the PTZ/PTZ$^+$, Ru^{2+}/Ru$^+$, Ru$^+$/Ru^0, and Ru^0/Ru$^-$ processes, respectively. Each redox process had the correct potential, and each process was fully chemically reversible (i.e., $i_{pa}/i_{pc} = 1.0$). Only samples exhibiting no other redox processes within the potential range scanned were used in the time-resolved emission studies.

[Ru(4*p*-PTZ)$_2$(DMB)](PF$_6$)$_2$, [Ru(4*p*-PTZ)$_2$(bipyridine)](PF$_6$)$_2$, and [Ru(4*p*-PTZ)$_2$(TMB)](PF$_6$)$_2$. These donor−chromophore complexes were prepared and characterized in the same manner as that described for [Ru(bpy, DMB, or TMB)$_2$(4*p*-PTZ)](PF$_6$)$_2$ using 1 equiv of Ru(4*p*-PTZ)$_2$Cl$_2$ and 1 equiv of bpy, DMB, or TMB.

The cyclic voltammetric peak currents for the respective oxidation or reduction waves indicate a ratio of 2:1:1:1 for the PTZ/PTZ$^+$, Ru^{2+}/Ru$^+$, Ru$^+$/Ru^0, and Ru^0/Ru$^-$ processes, respectively. As was found for the RuL$_2$(4*p*-PTZ)$^{2+}$ complexes, each redox process had the correct potential and each was fully chemically reversible.

[Ru(4*p*-PTZ)$_3$]$^{2+}$. The 4*p*-PTZ ligand (5 equiv) was placed in a nitrogen-flushed 100 mL round-bottom flask containing a magnetic stirring bar and 60 mL of ethanol. From this point on, room light was rigorously excluded. Ru(DMSO)$_4$Cl$_2$ (1 equiv, 30 mg) was dissolved in 2−3 mL of distilled water and this solution was added by thirds over 30-min intervals to the refluxing ethanol solution of 4*p*-PTZ. After addition of all of the Ru^{2+} solution the reaction was heated at reflux for an additional 2 h. The reaction mixture was cooled to room temperature, and the ethanol and water were removed by rotary evaporation. The remaining solid was purified by column chromatography on silica gel (eluent: 10% saturated aqueous KNO_3/40% water/50% acetonitrile). The mobile orange fractions were combined and filtered, and saturated NH_4PF_6 (2 mL) was added. The solvent was reduced in volume by rotary evaporation until the orange solid coated the side of the flask. The remaining uncolored solvent was decanted. The residue was dissolved in a minimum of acetonitrile and added dropwise to a centrifuge tube containing 50 mL of ethyl ether. The product (as a solid or oil, depending on the value of *p*) was isolated by

(40) Larson, S. L.; Elliott, C. M.; Kelley, D. F. *J. Phys. Chem.* **1995**, *99*, 6530.

centrifugation and washed with 3 × 50 mL of hot toluene to remove unreacted ligand. The precipitation from ethyl ether was repeated, and the product was isolated by centrifugation and dried *in vacuo* for 12 h at room temperature (yield approximately 80%).

Peak current ratios from cyclic voltammetry were 3:1:1:1 for the PTZ^0/PTZ^+, Ru^{2+}/Ru^+, Ru^+/Ru^0, and Ru^0/Ru^- processes, respectively. Each redox process had the expected potential, and each was fully chemically reversible.

Determination of Sample Integrity. The integrity of these light- and air-sensitive donor−chromophore complexes was determined by a combination of methods. Elemental analysis has been performed on some samples, but as we found with related C−A and D−C−A complexes,[40] such analyses are not especially useful in determining the integrity of a complex *vis-á-vis* time-resolved spectral analysis. For example, samples which have yielded entirely acceptable C, H, and N analysis values have proved to be impure by electrochemical and spectral criteria and *vice versa*. The failure of classical elemental analysis to adequately evaluate sample integrity, in this context, probably stems from a combination of the large molecular weight of the complexes and the fact that the complexes are unstable in the presence of both light and oxygen. In practice, a combination of chromatographic, electrochemical, and spectral analysis proved to be much more dependable in establishing sample integrity for time-resolved studies.

Each of the donor−chromophore complexes was purified by repeated water-washed silica gel column chromatography (eluent: 10% saturated aqueous KNO_3/40% water/50% acetonitrile) until they yielded UV−visible spectra which did not change with further chromatographic purification (impure samples have broad absorptions throughout the UV region and a shoulder at about 500 nm). Thus, the initial criterion of purity was the exact superposition of the spectrum throughout the UV and visible regions with scaled spectra of complexes exhibiting good electrochemistry, clean TLC, and single-exponential decays in the time-resolved emission spectroscopy (*vide infra*).

Emission Spectra and Time-Correlated Single-Photon Counting System. Steady-state luminescence spectra were obtained as described elsewhere.[41a] Emission onset energies were approximated by extrapolation of the inflection point of emission spectra (at room temperature) back to the wavelength axis.

The time-correlated single-photon counting (TCSPC) apparatus consists of a picosecond laser system, light detection system, and TCSPC electronics and has been described in the literature.[41] This apparatus was based on a picosecond laser/time-correlated single-photon counting system using a CW mode-locked Nd-YAG laser. The dye laser output (ca. 100 mW, used at 630 nm) was doubled (315 nm, ∼10 ps) and focused to ca. 0.5 nm for sample excitation. Sample emission was collected and focused through a $^1/_4$ m monochromator with a 150 groove/mm grating. A Hamamatsu microchannel plate photomultiplier (#R2809) (MCP PMT) was used for detection. In the single-photon counting electronics, the MCP PMT signal was amplified, attenuated, amplified again, and fed into one channel of a Tennelec TC 454 constant-fraction discriminator (CFD). This pulse from the CFD was used to "start" an Ortec 457 time-to-amplitude converter (TAC). The "stop" pulse was provided by another channel of the CFD, triggered by the output of a Hewlett-Packard 4023 photodiode which detects pulses of the dye laser fundamental. Output from the TAC was fed into a multichannel analyzer/computer for analysis. The temporal response of the instrument was generally ca. 70 ps.

Preparation of Samples for Kinetic Studies. Solid samples of all the complexes were either kept rigorously in the dark or stored in a drybox (Vacuum Atmospheres Corp.) under an N_2 atmosphere to prevent photodecomposition in the presence of oxygen. Samples were prepared in the drybox. A small quantity (ca. 2 mg) was transferred to a sample tube, consisting of a 2 mm path length quartz cell attached to a Pyrex tube sealed with a Kontes Teflon-and-glass valve. Sample tubes were then sealed in the drybox, wrapped in aluminum foil, removed from the drybox, placed on a vacuum line outside the drybox, and evacuated for about 5 min ($<5 \times 10^{-3}$ Torr). A portion of the desired solvent (1,2-dichloroethane, Aldrich reagent grade; acetonitrile, J. T. Baker Photorex; both used without further purification) was then degassed by three to five cycles of freeze−pump−thaw and distilled into a Pyrex sidearm of the sample cell. Two more freeze−pump−thaw cycles were then performed, and the sample tubes were sealed under vacuum. Samples were stored in the dark. Immediately before analysis the samples were frozen, evacuated, thawed, and warmed to room temperature.

(41) (a) Brucker, G. A.; Kelley, D. F. *J. Phys. Chem.* **1987**, *9*, 2856. (b) Nimlos, M. R.; Young, M. A.; Bernstein, E. R.; Kelley, D. F. *J. Am. Chem. Soc.* **1989**, *91*, 5269.

Table 1. Voltammetrically Determined $E_{1/2}$ Values for the PTZ(+/0) Process[a]

phenothiazine ligand (4*p*-PTZ)	uncoordinated ligand	donor−chromophore complex $[Ru(4p\text{-}PTZ)_2DMB]^{2+}$
Me-PTZ	0.650	
41-PTZ	0.800	0.853
43-PTZ	0.740	0.760
44-PTZ	0.686	0.700
45-PTZ	0.692	0.702
46-PTZ	0.683	0.696
47-PTZ	0.684	0.704
48-PTZ	0.683	0.694

[a] Values are in V vs SCE and were obtained in 0.1 M $(TBA)PF_6$/acetonitrile at a glassy-carbon electrode. The scan rate was 100 mV/s.

Table 2. Voltammetrically Determined $E_{1/2}$ Values for RuL_3 Complexes[a]

complex	PTZ(+/0)	Ru(2+/+)
$Ru(DMB)_3$		−1.37
$Ru(bpy)_2(44\text{-}PTZ)$	+0.70	−1.31
$Ru(bpy)(44\text{-}PTZ)_2$	+0.70	−1.34
$Ru(44\text{-}PTZ)_3$	+0.70	−1.40
$Ru(TMB)_2(44\text{-}PTZ)$	+0.70	−1.51
$Ru(TMB)(44\text{-}PTZ)_2$	+0.70	−1.46
$Ru(bpy)_2(47\text{-}PTZ)$	+0.70	−1.31
$Ru(bpy)(47\text{-}PTZ)_2$	+0.70	−1.34
$Ru(47\text{-}PTZ)_3$	+0.70	−1.40
$Ru(TMB)_2(47\text{-}PTZ)$	+0.70	−1.51
$Ru(TMB)(47\text{-}PTZ)_2$	+0.70	−1.46
$Ru(43\text{-}PTZ)_n(DMB)_{3-n}$	+0.76	−1.40
$Ru(44\text{-}PTZ)_n(DMB)_{3-n}$	+0.70	−1.41
$Ru(45\text{-}PTZ)_n(DMB)_{3-n}$	+0.70	−1.39
$Ru(46\text{-}PTZ)_n(DMB)_{3-n}$	+0.70	−1.40
$Ru(47\text{-}PTZ)_n(DMB)_{3-n}$	+0.70	−1.40
$Ru(48\text{-}PTZ)_n(DMB)_{3-n}$	+0.70	−1.39

[a] Values are in V vs SCE and were obtained in 0.1 M $(TBA)PF_6$/acetonitrile at a glassy-carbon electrode. The scan rate was 100 mV/s.

Results

Electrochemical Results. $E_{1/2}$ values (from cyclic voltammetry) of phenothiazine-containing ligands and the corresponding ruthenium complexes are reported in Tables 1 and 2. When the number of methylenes in the chain connecting the bipyridine and phenothiazine moieties, *p*, is 4 or greater, the electrochemistry is seen to be chain length independent. When PTZ is complexed to RuL_3^{2+}, its oxidation is at slightly more positive potentials than for the free ligand. The effect is most pronounced for the ligands having the shortest alkyl linkages. All processes reported are fully reversible.

Ground-State Absorption Spectra. The static absorption spectrum of $Ru(bpy)_3^{2+}$ is characterized by intense bands in the UV and visible regions. The bands observed at around 300 nm correspond to the bipyridine $\pi-\pi^*$ transitions, and the band in the visible region corresponds to the RuL_3^{2+} metal-to-ligand charge transfer (MLCT) transition (460 nm). The ligands containing a phenothiazine donor absorb below 330 nm when uncoordinated; when they are coordinated in the D−C complexes, an increased absorbance up to 390 nm is observed. This increased absorbance is independent of the chain length separating the donor and chromophore. Figure 2 shows the UV−vis spectra for methylphenothiazine, $Ru(DMB)_3$, and the series $Ru(44\text{−}PTZ)_N(DMB)_{N-3}$ in 1,2-dichloroethane (DCE).

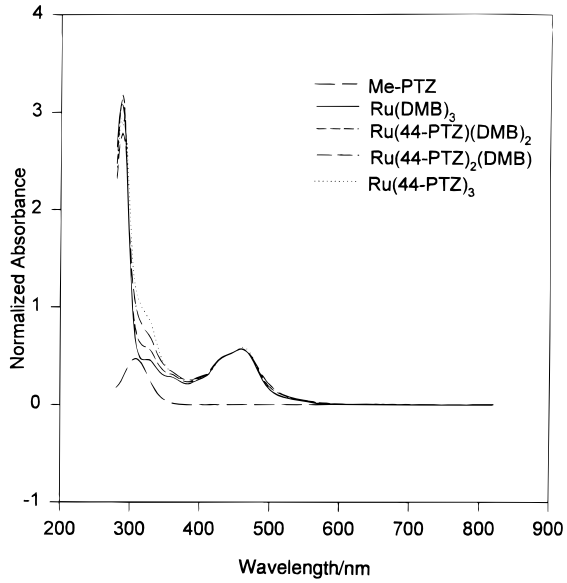

Figure 2. UV−vis spectra in DCE of phenothiazine-containing complexes.

Table 3. Emission Onset for Donor−Chromophore Complexes at Room Temperature

complex	ACN in nm (eV)	DCE in nm (eV)
Ru(bpy)$_2$(44-PTZ)	563 (2.20)	558 (2.22)
Ru(bpy)(44-PTZ)$_2$	567 (2.19)	564 (2.20)
Ru(44-PTZ)$_3$	563 (2.20)	557 (2.23)
Ru(TMB)$_2$(44-PTZ)	570 (2.17)	557 (2.23)
Ru(TMB)(44-PTZ)$_2$	567 (2.19)	564 (2.20)
Ru(bpy)$_2$(47-PTZ)	565 (2.20)	559 (2.22)
Ru(bpy)(47-PTZ)$_2$	568 (2.18)	563 (2.20)
Ru(47-PTZ)$_3$	563 (2.20)	557 (2.23)
Ru(TMB)$_2$(47-PTZ)	567 (2.19)	557 (2.23)
Ru(TMB)(47-PTZ)$_2$	568 (2.18)	563 (2.20)

Emission onsets following excitation at 460 nm are reported in Table 3. Emission from donor−chromophore complexes is diminished compared to that of the analogous chromophore without attached quenchers. The normalized emission of Ru(DMB)$_3^{2+}$ and that of Ru(44-PTZ)$_3^{2+}$ are superimposable in acetonitrile and are nearly so in DCE.

Emission decay curves were measured for the donor−chromophore complexes, and the emission decay rates are listed in Tables 4−6. Also listed in Tables 4−6 are the emission decay rates for complexes of ruthenium with variously methylated bipyridines. Decay curves were obtained following excitation at 315 nm, near the $\pi-\pi^*$ maximum, and MLCT emission was monitored in the red region of the spectrum. The onset of MLCT emission is in the range of 550−570 nm, with a maximum at ca. 620 nm. In all cases, decay curves were obtained by monitoring at 630 nm. No systematic variation in the characteristics of these decay curves was found in the 550−800 nm range.

A representative emission decay curve is shown in Figure 3, measured for [Ru(44−PTZ)$_3$]$^{2+}$ in dichloroethane. The emission kinetics can be fit to a single-exponential decay with a small percentage of long-time constant component. The percentage of constant component varies among samples. The values for decay times given in Tables 4−6 refer to the exponential decay component. For all the donor−chromophore complexes in dichloroethane and acetonitrile, fits were greater than 90% single exponentials. These samples are extremely sensitive to air and light; careful purification leads to a decrease in the long-lived emission, but it is very difficult to eliminate entirely. However, the fact that its magnitude varies between sample preparations and that it constitutes only a small fraction of the total emission makes us comfortable in assigning this slowly decaying component to a luminescent impurity or impurities.

Table 4. Emission Decay[a] and Electron-Transfer[b] Rates (s^{-1}) for Donor−Chromophore Complexes in Dichloroethane (DCE) and Acetonitrile (ACN)

	emission decay		electron transfer	
complex	DCE	ACN	DCE	ACN
Ru(DMB)$_2$(43-PTZ)	7.3e^{+6} [c]	4.0e^{+6}	6.1e^{+6}	2.8e^{+6}
Ru(DMB)$_2$(44-PTZ)	6.6e^{+6}	3.9e^{+6}	5.4e^{+6}	2.7e^{+6}
Ru(DMB)$_2$(45-PTZ)	5.6e^{+6}	4.0e^{+6}	4.4e^{+6}	2.8e^{+6}
Ru(DMB)$_2$(46-PTZ)	4.1e^{+6}	4.0e^{+6}	2.9e^{+6}	2.8e^{+6}
Ru(DMB)$_2$(47-PTZ)	3.5e^{+6}	3.9e^{+6}	2.3e^{+6}	2.7e^{+6}
Ru(DMB)$_2$(48-PTZ)	3.2e^{+6}	3.9e^{+6}	2.0e^{+6}	2.7e^{+6}
Ru(DMB)(43-PTZ)$_2$	1.1e^{+6}	7.7e^{+6}	9.8e^{+6}	6.5e^{+6}
Ru(DMB)(44-PTZ)$_2$	1.2e^{+7}	7.2e^{+6}	1.1e^{+7}	6.0e^{+6}
Ru(DMB)(45-PTZ)$_2$	7.8e^{+6}	5.7e^{+6}	6.6e^{+6}	4.5e^{+6}
Ru(DMB)(46-PTZ)$_2$	6.4e^{+6}	6.9e^{+6}	5.2e^{+6}	5.7e^{+6}
Ru(DMB)(47-PTZ)$_2$	6.0e^{+6}	7.1e^{+6}	4.8e^{+6}	5.9e^{+6}
Ru(DMB)(48-PTZ)$_2$	4.0e^{+6}	5.7e^{+6}	2.8e^{+6}	4.5e^{+6}
Ru(43-PTZ)$_3$	2.7e^{+7}	1.3e^{+7}	2.6e^{+7}	1.2e^{+7}
Ru(44-PTZ)$_3$	2.0e^{+7}	1.3e^{+7}	1.9e^{+7}	1.2e^{+7}
Ru(45-PTZ)$_3$	1.8e^{+7}	1.4e^{+7}	1.7e^{+7}	1.3e^{+7}
Ru(46-PTZ)$_3$	1.6e^{+7}	1.3e^{+7}	1.5e^{+7}	1.2e^{+7}
Ru(47-PTZ)$_3$	7.2e^{+6}	9.8e^{+6}	6.0e^{+6}	8.6e^{+6}
Ru(48-PTZ)$_3$	7.7e^{+6}	9.4e^{+6}	6.5e^{+6}	8.2e^{+6}

[a] The observed rate of emission decay measured by time-resolved single-photon counting. [b] The electron-transfer rate calculated by subtracting the nonradiative decay rate from the observed emission decay rate. [c] In this table and in Tables 5 and 6, e^{+6} = 10^6, e^{+7} = 10^7, etc.

Table 5. Emission Decay[a] and Electron-Transfer[b] Rates for Donor−Chromophore Complexes and Analogous Chromophores in DCE

complex	emission decay rate (s^{-1})	electron-transfer rate (s^{-1})	electron-transfer rate per PTZ (s^{-1})	driving force (eV)[c]
Ru(bpy)$_2$(DMB)	1.1e^{+6}			
Ru(bpy)(DMB)$_2$	1.0e^{+6}			
Ru(DMB)$_3$	1.2e^{+6}			
Ru(TMB)(DMB)$_2$	1.2e^{+6}			
Ru(TMB)$_2$(DMB)	1.1e^{+6}			
Ru(bpy)$_2$(44-PTZ)	3.3e^{+7}	3.2e^{+7}	3.2e^{+7}	+0.21
Ru(bpy)(44-PTZ)$_2$	2.5e^{+7}	2.4e^{+7}	1.2e^{+7}	+0.16
Ru(44-PTZ)$_3$	2.0e^{+7}	1.9e^{+7}	6.3e^{+6}	+0.12
Ru(DMB)(44-PTZ)$_2$	1.2e^{+7}	1.1e^{+7}	5.4e^{+6}	+0.12
Ru(DMB)$_2$(44-PTZ)	6.6e^{+6}	5.4e^{+6}	5.4e^{+6}	+0.12
Ru(TMB)$_2$(44-PTZ)	1.4e^{+6}	2.0e^{+5}	2.0e^{+5}	+0.01
Ru(TMB)(44-PTZ)$_2$	6.3e^{+6}	5.1e^{+6}	2.6e^{+6}	+0.04
Ru(bpy)$_2$(47-PTZ)	1.6e^{+7}	1.5e^{+7}	1.5e^{+7}	+0.21
Ru(bpy)(47-PTZ)$_2$	1.3e^{+7}	1.2e^{+7}	6.0e^{+6}	+0.16
Ru(47-PTZ)$_3$	7.2e^{+6}	6.0e^{+6}	2.0e^{+6}	+0.12
Ru(DMB)(47-PTZ)$_2$	6.0e^{+6}	4.8e^{+6}	2.4e^{+6}	+0.12
Ru(DMB)$_2$(47-PTZ)	3.5e^{+6}	2.3e^{+6}	2.3e^{+6}	+0.12
Ru(TMB)$_2$(47-PTZ)	1.4e^{+6}	2.0e^{+5}	2.0e^{+5}	+0.01
Ru(TMB)(47-PTZ)$_2$	1.9e^{+6}	7.1e^{+5}	3.6e^{+5}	+0.04

[a] The observed rate of emission decay measured by time-resolved single-photon counting. [b] The electron-transfer rate calculated by subtracting the nonradiative decay rate from the observed emission decay rate. [c] $-\Delta G$ of ET reaction.

Discussion

The emission decay rates presented in Tables 4−6 can be used to obtain donor−chromophore electron transfer rates. In general, the emission decay rate is given by the sum of radiative and nonradiative decay rates and the electron-transfer rate. The sum of the radiative and nonradiative decay rates is well approximated by the emission decay rate in corresponding complexes which lack a phenothiazine quencher. For this

Table 6. Emission Decay[a] and Electron-Transfer[b] Rates for Donor−Chromophore Complexes and Analogous Chromophores in Acetonitrile

complex	emission decay rate (s^{-1})	electron-transfer rate (s^{-1})	electron-transfer rate per PTZ (s^{-1})	driving force (eV)[c]
$Ru(bpy)_2(DMB)$	$1.0e^{+6}$			
$Ru(bpy)(DMB)_2$	$1.1e^{+6}$			
$Ru(DMB)_3$	$1.2e^{+6}$			
$Ru(TMB)(DMB)_2$	$1.3e^{+6}$			
$Ru(TMB)_2(DMB)$	$1.3e^{+6}$			
$Ru(bpy)_2(44\text{-}PTZ)$	$3.3e^{+7}$	$1.2e^{+7}$	$1.2e^{+7}$	+0.19
$Ru(bpy)(44\text{-}PTZ)_2$	$1.2e^{+7}$	$1.1e^{+7}$	$5.5e^{+7}$	+0.15
$Ru(44\text{-}PTZ)_3$	$1.3e^{+7}$	$1.2e^{+7}$	$3.9e^{+6}$	+0.10
$Ru(DMB)(44\text{-}PTZ)_2$	$7.2e^{+7}$	$6.0e^{+7}$	$3.0e^{+6}$	+0.10
$Ru(DMB)_2(44\text{-}PTZ)$	$3.9e^{+6}$	$2.7e^{+6}$	$2.7e^{+6}$	+0.10
$Ru(TMB)_2(44\text{-}PTZ)$	$1.5e^{+6}$	$2.0e^{+5}$	$2.0e^{+5}$	−0.04
$Ru(TMB)(44\text{-}PTZ)_2$	$3.4e^{+6}$	$2.1e^{+6}$	$1.1e^{+6}$	+0.03
$Ru(bpy)_2(47\text{-}PTZ)$	$1.4e^{+7}$	$1.3e^{+7}$	$1.3e^{+7}$	+0.20
$Ru(bpy)(47\text{-}PTZ)_2$	$1.3e^{+7}$	$1.2e^{+7}$	$6.0e^{+6}$	+0.16
$Ru(47\text{-}PTZ)_3$	$9.8e^{+6}$	$8.6e^{+6}$	$2.9e^{+6}$	+0.10
$Ru(DMB)(47\text{-}PTZ)_2$	$7.1e^{+6}$	$5.9e^{+6}$	$2.9e^{+6}$	+0.10
$Ru(DMB)_2(47\text{-}PTZ)$	$3.9e^{+6}$	$2.7e^{+6}$	$2.7e^{+6}$	+0.10
$Ru(TMB)_2(47\text{-}PTZ)$	$1.6e^{+6}$	$3.0e^{+5}$	$3.0e^{+5}$	−0.02
$Ru(TMB)(47\text{-}PTZ)_2$	$2.5e^{+6}$	$1.2e^{+5}$	$6.0e^{+5}$	+0.02

[a] The observed rate of emission decay measured by time-resolved single-photon counting. [b] The electron-transfer rate calculated by subtracting the nonradiative decay rate from the observed emission decay rate. [c] $-\Delta G$ of ET reaction.

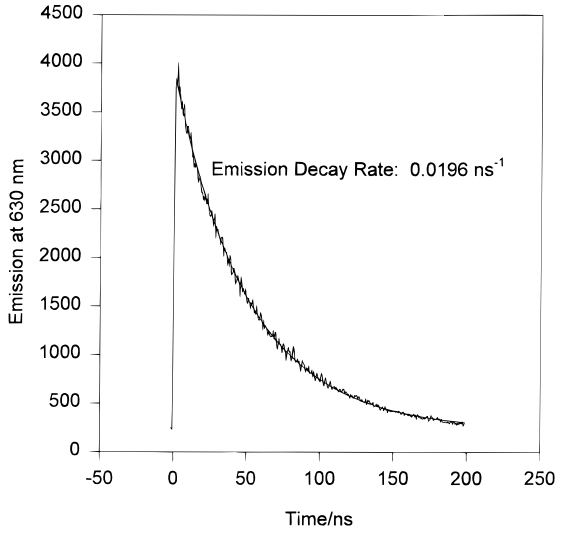

Figure 3. Emission decay at 630 nm for $[Ru(44\text{-}PTZ)_3]^{2+}$ obtained in DCE solvent. The smooth line is the calculated fit.

purpose, the phenothiazine-containing ligands are approximated by 4,4′-dimethylbipyridine (DMB). The electron-transfer rates are also presented in Tables 4−6.

Three general observations are evident from examination of these electron-transfer rates. First, the rates decreased with increasing numbers of methylenes in the linkage for DCE solvent but not for acetonitrile. Second, when the driving force is held constant (i.e. complexes containing only DMB and phenothiazine-containing ligands), the rate of electron transfer increases linearly with the number of phenothiazine-containing ligands in the complexes. Finally, for donor−chromophore complexes, the magnitude of the ET driving force, and hence the quenching rate, decreases with the extent of methyl substitution of the bipyridine ligands. These observations are discussed below.

Linkage Dependence. Figure 4 shows the dependence of electron-transfer rate, for the $[Ru(DMB)_2(4p\text{-}PTZ)]^{2+}$ series in DCE, on the number of bridging methylene groups, *p*. A

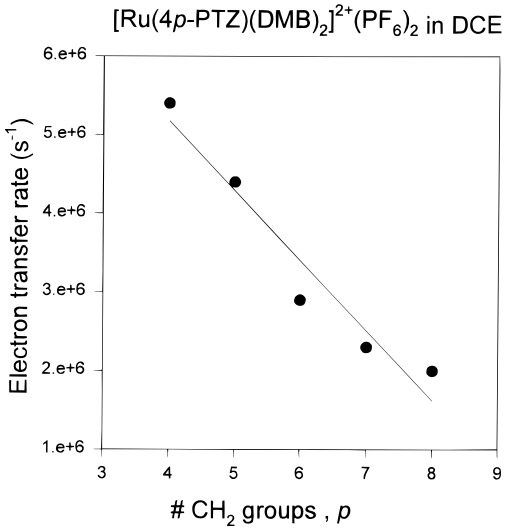

Figure 4. Electron-transfer rate versus the number of CH_2 groups, *p*, for $[Ru(4p\text{-}PTZ)(DMB)_2](PF_6)_2$.

roughly linear relationship is observed between *p* and electron-transfer rate. In electron-transfer systems where rigid spacers separate the reactants, an exponential dependence on separation is usually observed.[22−29] This exponential decrease in ET rate is due to the exponential decrease in orbital overlap with distance between the donor and acceptor. In many cases, the donor−acceptor interaction is dominated by superexchange through the rigid σ framework. We have demonstrated previously, for a series of analogous donor−chromophore−acceptor (D−C−A) complexes (also having flexible linkages) that through-σ-bond superexchange appears not to be the dominant mechanism of electron transfer.[40] The linear dependence of the quenching rate in DCE on the value of *p* for the present complexes can similarly be rationalized best in terms of the role of chain dynamics in the electron-transfer process.

In these flexibly-linked donor−chromophore complexes the physical separation of the reactants changes rapidly on the time scale of the electron transfer (40−200 ns). This results in a spacial distribution of PTZ donors relative to the Ru^{2+} chromophore at a given instant. This distribution contains some fraction of complexes in which the donor and chromophore have sufficient orbital overlap for electron transfer to take place. As the chain length increases, the volume accessed by the phenothiazine also increases, but the volume in which sufficient orbital overlap exists for electron transfer remains approximately the same. Thus, the relative number of phenothiazines in close proximity to the chromophore decreases as the chain length increases, and as a consequence, so does the rate of quenching.

As can be seen in Table 4, in contrast to the results in DCE no appreciable dependence on the chain length, *p*, is observed in acetonitrile solvent. These results are similar to what has been observed by Winnick *et al.*[42] for a series of alkyl-linked anthracene-alkylamines. These investigators observed only a weak dependence of electron transfer rate on the chain length in polar solvents and a greatly increased dependence on nonpolar solvents. The fact that chain length dependence is observed in nonpolar solvents and not in polar solvents can be rationalized in terms of the extent of chain extension resulting from the differences in "solubility" of the alkyl chain in the two media. The aliphatic chain is highly soluble in nonpolar solvents and, consequently, it is more likely to be able to accesses the full range of possible conformations. In polar solvent, however, the alkyl chains are less soluble and, thus, would be more prone to fold back upon themselves, resulting in a smaller range of

(42) Winnik, M.; Zachariasse, K. J. *J. Phys. Chem.* **1984**, *88*, 2964.

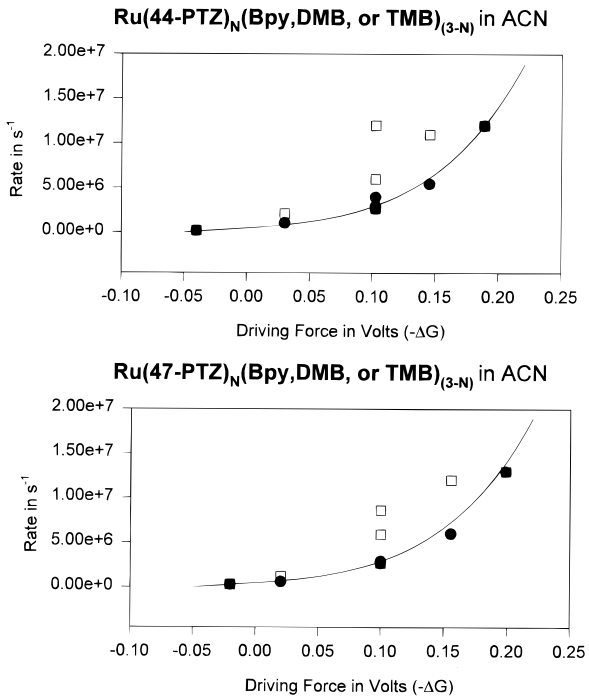

Figure 5. ET rate versus driving force for donor−chromophore complexes in acetonitrile (ACN). The open squares are the data reported in Table 6; the solid circles are the same data normalized for the number of PTZ quenchers per molecule.

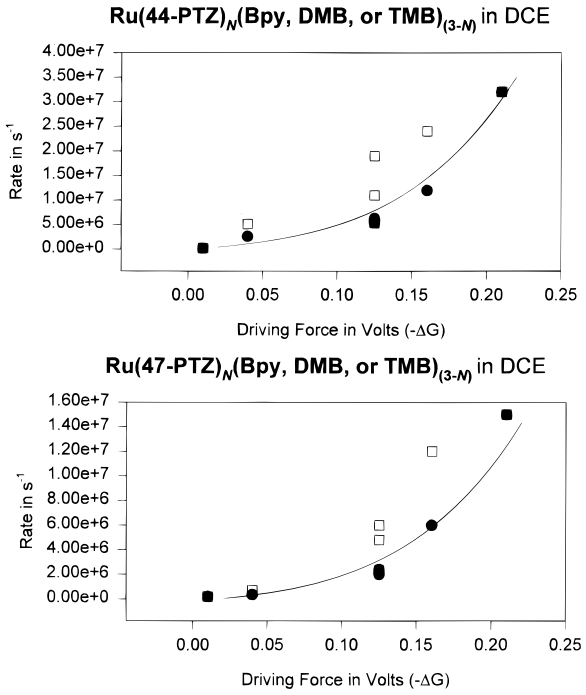

Figure 6. ET rate versus driving force for donor−chromophore complexes in dichloroethane (DCE). The open squares are the data reported in Table 5; the solid circles are the same data normalized for the number of PTZ quenchers per molecule.

donor−chromophore distances. A similar explanation has been used to rationalize solvent effects in organic reactions where conformational motions of alkyl chains are also important.[43]

Dependence on Number of Phenothiazine-Containing Ligands. The data in Tables 4−6 allow a comparison of the electron-transfer rates for complexes in which the same chain length separates the phenothiazine(s) and the chromophore but differing numbers of phenothiazine-containing ligands are present. Consideration of the ET rates for the complexes [Ru(4*p*-PTZ)$_N$(DMB)$_{3-N}$], where *p* is constant and $N = 1$, 2, or 3, shows that the rates are approximately proportional to the value of *N*, indicating that each phenothiazine quenches the MLCT state independently. This behavior is observed to be independent of the solvent.

Dependence on Driving Force and Remote Ligands. The driving forces for quenching of the RuL_3 MLCT state by the covalently attached phenothiazine donors are small (−0.02 to +0.21 V) and depend on the oxidation potential of the phenothiazine, the reduction potential of the ruthenium ($Ru^{2+/+}$), and the excited-state energy of Ru^{2+*}. Specifically, the driving force for the quenching process can be estimated from

$$\Delta G \simeq E_{1/2}(\mathrm{PTZ}^{+/0}) - E_{1/2}(\mathrm{Ru}^{2+/+}) - E(\mathrm{MLCT}) \quad (1)$$

where the $E_{1/2}$ values are obtained electrochemically (Table 2) and *E*(MLCT) is the onset of MLCT emission (Table 3). The calculated driving forces are reported in the last columns of Tables 5 and 6. The small driving forces involved make the possible errors in measuring either the redox potentials or the emission onsets significant. As a result, any single piece of data cannot be taken as providing insight into the dynamics of the quenching process. That caveat notwithstanding, the general trends in how the electron-transfer rates vary with the estimated driving force are informative.

Figures 5 and 6 show the dependence of the electron-transfer rate on the driving force in acetonitrile and DCE, respectively. Also included in each figure are the rates calculated from Marcus theory (solid line). The squares are the measured electron-transfer rates reported in Tables 4 and 5. The solid circles are the same rates normalized for the number of phenothiazine quenchers present per complex. Once normalized, for a set of isoenergetic complexes, Ru(L)$_N$(4*p*-PTZ)$_{3-N}$, the effective (i.e. per phenothiazine) rates are identical within experimental error and all agree with the values predicted by Marcus' theories. The dependence of the electron transfer rate on driving force is given by

$$k_2 = A \exp\left(\frac{-\Delta G^{\ddagger}}{RT}\right) \quad (2)$$

where *A* is a constant which can be taken to be the same for donor−chromophore complexes with the same value of *p* in the same solvent. The value of $\Delta G^{\ddagger}$ is given by Marcus theory. Specifically

$$\Delta G^{\ddagger} = \frac{\lambda}{4}\left(1 + \frac{\Delta G}{\lambda}\right)^2 \quad (3)$$

where ΔG is the reaction exothermicity and λ is the reorganization energy. We have previously shown that the reorganizational energy is largely outer sphere in nature for these systems.[37]

The calculated curves in Figures 5 and 6 were obtained using solvent reorganization energies of 0.8 and 0.7 V, respectively, for acetonitrile and DCE.[37] The value of *A* was taken to be an adjustable parameter. Estimates of ΔG were obtained from the electrochemical data acquired in acetonitrile, as listed in Tables 1 and 2, and the energy corresponding to the onset of emission in acetonitrile. Unfortunately, similar $E_{1/2}$ data cannot be obtained in DCE due to the potential limits of that solvent. Although ΔG may differ somewhat between the two solvents, those differences are expected to be small and should not affect the overall conclusions. Very good agreement between the observed rates and the calculated curve is obtained in both solvents.

Comparison with Donor−Chromophore−Acceptor Complexes. In recent publications the dynamics of charge-separated-state formation for donor−chromophore−acceptor (D−C−A) complexes were presented.[37,40] These complexes are identical

(43) van Tamelen, E. E.; Curphey, T. J. *Tetrahedron Lett. 3*, **1962**, 121.

Scheme 1

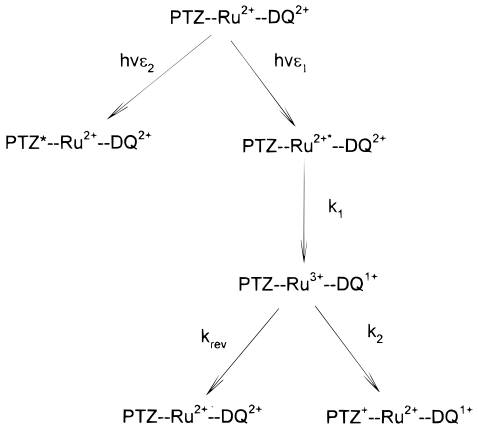

with the ones presently under consideration, except that one of the DMB ligands is replaced by a bipyridine linked to a diquaternary amine electron acceptor. Unlike the D−C complexes considered here, upon photexcitation, the D−C−A complexes form long-lived charge-separated states (CS) in DCE solvent. In the CS state the donor is oxidized, the acceptor is reduced, and the RuL_3 chromophore is returned to its ground state. Scheme 1 presents the mechanism by which the charge-separated state is formed. In these D−C−A complexes, the MLCT excitation is quenched by Ru^{2+}*-to-acceptor ET. Subsequently, either recombination (acceptor-to-Ru^{3+} ET, k_{rev}) or charge separation (PTZ-to-Ru3+ ET, k_2) occurs. The quantum yield for CS formation is thus determined by the relative magnitudes of k_{rev} and k_2 in Scheme 1. It is important to note that the rate of recombination, k_{rev}, should be independent of the donor ligand and dependent only on the acceptor ligand, since the reaction involves only the Ru^{3+} and the reduced acceptor. Thus, for a D−C−A complex containing a given acceptor ligand, the quantum yield will vary only with k_2 and for a given k_{rev} the ratio k_2/k_{rev} can be obtained.

The CS state quantum yield and k_2/k_{rev} have been determined for two series of D−C−A complexes, $[Ru(4p\text{-}PTZ)_2(423\text{-}DQ^{2+})]^{4+}$ and $[Ru(4p\text{-}PTZ)_2(424\text{-}DQ^{2+})]^{4+}$, where $p = 3-8$ and 423-DQ^{2+} and 424-DQ^{2+} are acceptor-containing ligands.[40] These rates may be compared with those obtained in the corresponding donor−chromophore complexes reported here.

Before making that comparison, some discussion of the D−C−A results is in order. The detailed analysis of these results is presented elsewhere;[40] however, the pertinent conclusions can be summarized as follows: on the basis of, primarily, the acceptor−chromophore linkage dependence of CS-state formation, it was determined that the rates of both recombination and CS-state formation must be fast relative to any large-scale conformational motion of either the acceptor or the phenothiazine donor. Consequently, k_2 in Scheme 1 does not represent a single rate constant but rather a distribution of rate constants which reflects the statistical distribution of PTZ-to-Ru^{3+} distances at the instant the initial quenching event occurs. Thus, as p increases, the relative fraction of PTZ donors that are within electron-transfer distance decreases, resulting in a smaller effective value of k_2.

Figure 7 is a plot of the ET rates from Table 4 for the donor−chromophore complexes vs relative values of k_2 for analogous D−C−A complexes reported in ref 40. The driving forces for electron transfer in the latter case can be calculated from electrochemical measurements and are fairly large (ca. 400 mV), commensurate with the fast rate of CS state formation. As can be seen from the data in Figure 7, there is a linear relationship between these two sets of rate constants, implying a similar

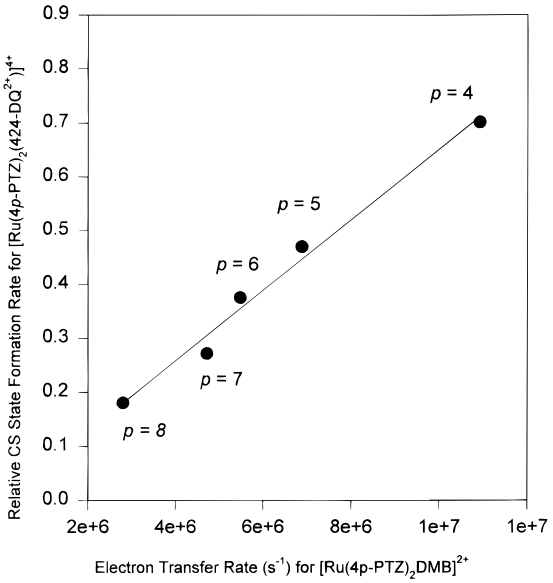

Figure 7. Relative rates of charge-separated-state formation (k_2/k_{rev}; Scheme 1) for D−C−A complexes vs donor−chromophore electron-transfer rate: $[Ru(4p\text{-}PTZ)_2(424\text{-}DQ^{2+})]^{4+}$ measured in DCE.

dependence on linkage for both electron-transfer reactions (i.e. PTZ-to-Ru^{3+} and PTZ-to-Ru^{2+}*). In the latter case the ET is slow relative to conformational motions, and in the former case, it is fast. In both cases the distribution of donor−chromophore distances is not perturbed by the respective electron transfer. When electron transfer is very slow, rapid conformation motions maintain the equilibrium distribution. In the other extreme, the competition between the k_2 and k_{rev} electron-transfer processes is sufficiently fast that ET takes a "snapshot" of the unperturbed distribution. Consequently, it is reasonable that both rate constants appear to have the same relative dependence on the value of p.

Conclusion

The electron-transfer quenching of the RuL_3 MLCT excited state by attached PTZ donors is best explained by employing a model which considers an equilibrium distribution of chromophore−donor distances. This distribution is enforced by the methylene chain linking the two moieties together. The solvent dependence of the electron-transfer process is, likewise, rationalized on the basis of how the expected solubility of the polymethylene-chain linkage should influence the equilibrium distributions of D−C distances. Since quenching rates scale linearly with the numbers of PTZ donors present in a given complex, it is assumed that the donors are noninteracting. Also, electron-transfer rates normalized for the number of PTZ donors are fully consistent with normal Marcus theory when reasonable values for solvent reorganizational energies are employed. Finally, there is a strong correlation between the ET rate in these D−C complexes and the relative rate of CS-state formation in related D−C−A complexes.[40] These two processes, though quite different in absolute rates and degree of exothermicity, appear to exhibit the same type of D−C-linkage dependence. This correlation can also be explained by considering a distribution of distances enforced by D−C linkage.

Acknowledgment. This work was supported by (C.M.E.) the U. S. Department of Energy, Office of Basic Energy Sciences (Contract No. DE-FG02-92ER14301) and (D.F.K.) the National Science Foundation.

IC9504699